Chemical Physics 582 (2024) 112276

Contents lists available at ScienceDirect

Chemical Physics

journal homepage: www.elsevier.com/locate/chemphys

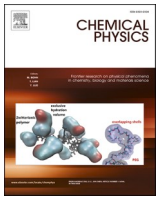

Interaction between chitosan and arsenic acid

Brandon Meza-González [a], Mariela Molina Jacinto [b], Leonardo Brito-Flores [a], Fernando Cortes-Guzman [a,*], Rosa María Gómez-Espinosa [b,*]

[a] Facultad de Química, Universidad Nacional Autónoma de México, Ciudad Universitaria, CDMX, 04510, Mexico
[b] Centro Conjunto de Investigación en Química Sustentable UAEM-UNAM, Carretera Km. 14.5, Unidad San Cayetano, Toluca - Atlacomulco, Toluca de Lerdo, México 50200, Mexico

ARTICLE INFO

Keywords:
Arsenic adsorption
Chitosan membrane
Molecular dynamics
Two-layer adsorption
Arsenic-arsenic interactions
Membrane design
Quantum chemistry topology analysis

ABSTRACT

We present a computational study of the adsorption of arsenic species onto a modified chitosan membrane. We found that absorbing arsenic onto a chitosan-modified membrane can be broken down into two steps: a weak hydrogen bonding occurs, followed by two-layer arsenic adsorption. The most stable arrangement is a one-side conformation, where arsenic interacts only in a certain side of the chitosan. Molecular dynamics simulations show the formation of two layers during arsenic adsorption: a primary layer with direct interactions between chitosan and arsenic molecules and a secondary layer where arsenic molecules interact with each other and the primary layer. The results of this work can be used in the context of membrane design.

1. Introduction

Arsenic is a natural component of the subsoil, but its presence in drinking water harms health [1]. Consumption of water contaminated with arsenic can cause cardiovascular, liver, hematological, neuronal, renal, and respiratory problems, and it is associated with different types of cancer (skin, lung, liver, and bladder) [2]. At least 8.81 million people have been exposed to arsenic concentrations above established limits (WHO established a limit of 10 g/L) [3,4]. The arsenic contamination comes from anthropogenic sources such as mining, agriculture, and carbon combustion processes or from natural processes, such as volcanic eruptions and weathering of rocks, which contain arsenic [5]. In Mexico, 40 % of the population is supplied with water from underground sources, where a large part of the aquifers are contaminated with arsenic in the semi-arid and arid areas of the center and north of the country.

Different arsenic removal techniques have been developed, ranging from precipitation processes, ion exchange, membrane filtration, coagulation, and flocculation. However, some of these have disadvantages, such as sludge generation, specialized labor requirements, or high maintenance costs [6]. Among these processes, adsorption methods are the most attractive since their associated materials are selective to specific contaminants [7].

The removal of arsenic using adsorption processes depends mainly on the structures and reactivity of the arsenic species. Arsenate (As(V)) is found in an aqueous medium as $H_2AsO_4^-$ in a pH range of 3 to 6, as $HAsO_4^{2-}$ between 8 and 10.5 while around 6 to 7, both species coexist; However, at pH = 2, the dominant species is H_3AsO_4, and after 12, AsO_3^{3-} is the only observed [8]. The adsorption methods can remove negatively charged species ($H_2AsO_4^-$/$HAsO_4^{2-}$) by electrostatic interaction with the adsorbent surface by two possible mechanics. External sphere mechanisms carry out adsorption by electrostatic interaction since metal ions interact only with the surface of the functionalized material and are absorbed into it. On the other hand, the adsorption of arsenates can also occur through internal sphere mechanisms where arsenate ions diffuse and form complexes inside the membranes [9,10].

Iron oxides, magnesium, aluminum, zinc, iron compounds, biocarbon, and clay minerals stand out among the materials used as adsorbents of arsenates. Polysaccharides such as cellulose, chitin, chitosan, alginate, pectin, and starch have also been used [11,12]. Chitosan is highlighted for its abundant availability, structural characteristics, nontoxicity, biocompatibility, and competitive arsenic removal from water [13]. Chitosan is a derivative of chitin obtained by the deacetylation process and is composed of β-(1 → 4)-2-acetamido-D-glucose and β-(1 → 4)-2-amino-D-glucose units. Chitosan has primary and secondary amino functional groups (–NH_2), acetamido groups (–CH_2CONH-), and hydroxyl groups (–OH) at the *C*2, C3, and C6 positions, respectively. The presence of these functional groups (amino and hydroxyl) makes chitosan an efficient material for removing arsenic from water; since these

* Corresponding authors.
E-mail addresses: fercor@unam.mx (F. Cortes-Guzman), rosamarigo@gmail.com (R.M. Gómez-Espinosa).

https://doi.org/10.1016/j.chemphys.2024.112276
Received 8 February 2024; Received in revised form 18 March 2024; Accepted 26 March 2024
Available online 1 April 2024

can be protonated in acidic media, generating electrostatic attraction between the arsenates and the protonated chitosan, however, at alkaline pH, electrostatic repulsions are generated, generating a decrease in the adsorption of arsenic [14]. The arsenic adsorption on chitosan occurs by electrostatic attraction from free electron pairs, ion exchange, diffusion processes, metal chelation, or complex formation [15]. However, the mechanism of As(V) sorption on chitosan-based materials remains controversial regarding elucidating the coordination mechanism of arsenic oxyanions and chitosan since this not only depends on the functional groups of chitosan. There are efforts to depict the interaction between arsenic species and inorganic surfaces [16–18] and chitosan [19–22]. Recently, our research group reported a new material (polypropylene-chitosan) that demonstrated the ability to remove arsenic (V). The efficiency of chitosan supported on a modified polypropylene membrane achieved 75 % removal. We also found that the adsorption capacity increased as the pH decreased, observing that at pH = 1, the greatest removal of As (V) [14].

This paper studies the intermolecular interaction between chitosan and arsenic species. We found that the process of absorbing arsenic onto a chitosan-modified membrane can be broken down into two steps: a weak hydrogen bonding occurs, followed by two-layer adsorption. This has been proven through static calculations and MD simulations. According to the results, the most stable arrangement is a one-side conformation, where arsenic interacts only in a certain side of the chitosan. The level of stability significantly depends on the number of [As]-[As] interactions present. The results can be used in the context of membrane design.

2. Computational methods

The interactions between arsenic and chitosan were studied in static and dynamic ways, using DFT and semi-empirical calculations to describe their evolution. The widely known structure for chitosan [23] is shown in Fig. 1.a), whereas the dimer model employed in this work is depicted in Fig. 1.b). Thus, before the DFT calculations, a conformer search was carried out using the CREST method for all the systems studied [24]. Then, the optimization calculations were performed using wB97X-D3/def2-TZVP [25] at the theoretical level and the implicit CPCM model for water [26] using Orca 5.0.3 [27]. wB97X-D3 has been proven helpful in studying polymer structure and polymer-substrate interactions with metal [28] and non-metal-containing molecules [29–31]. Similarly, def2-TZVP has demonstrated success in the simulation of polymeric systems [32,33]. We considered protonated states at pH = 1. García-García et al. [14] have shown that the highest adsorption capacity of As(V) is reached around pH 1. The Kohn-Sham orbitals of each optimized system were calculated and analyzed using AIMAll code [34] to obtain the system's molecular graphs and bond critical points properties, as defined by the Quantum Theory of Atoms in Molecules (QTAIM) [35].

The semi-empirical approach used the GFN1-xTB method [36] as implemented in CP2K 8.1 [37]. The extended tight binding formalism (xTB) is well known for its ability to predict structural changes in complex systems [38,39]. This method has found broad applications in polymer studies [40,41], specifically in exploring the hydrogen bond formation process [42] and chitosan structure interaction with diverse substrates [43,44].

Although the Chi-As interaction has been modeled using computational approaches to the best of our knowledge, a computational model that addresses the entire membrane-solute interaction is needed [10,21,45,46]. For this reason, a more complex model was proposed to analyze the dynamic interactions of the arsenic with the chitosan in a grafted state and solvent molecules to simulate the experimental results. The polypropylene membrane (PP) was modeled by an aliphatic chain containing 26 carbon atoms. Grafted to the membrane, three acrylate units were placed equidistantly and used as a bridge to bond six units of chitosan through the $–NH_2$ groups, as proposed by Adhikari *et al.* [47]. Finally, twelve H_3AsO_4 molecules were included in the calculations, along with 276 explicit water molecules and Cl^- atoms as counterions. The molecular dynamics (MD) trajectory was propagated 180 picoseconds in an NVT ensemble with a 1.0 fs time step. All the analyses over the trajectory were done employing CPPTRAJ [48], VMD [49], and Pymol [50].

3. Results and discussion

3.1. Chi-As interactions

Two kinds of chitosan-arsenic acid (Chi—[As]) interactions were considered for the electronic structure calculations. The first corresponds to a one-sided Chi—[As] interaction, in which the H_3AsO_4 molecules interact solely on one face of the organic rings. The other approximation is a both-side interaction, in which arsenic molecules interact on both sides of the chitosan monomers. Fig. 2 presents these two modes of interaction.

Fig. 3 presents the molecular graphs for Chi$(H_3AsO_4)_2$. A bond critical point (BCP), shown in orange in Fig. 3, refers to a saddle point in the electron density between two nuclei. The properties of a BCP are essential for identifying and classifying chemical bonds and interatomic reactions [51]. Not only that, but they also play a crucial role in calculating interaction energies [52–55]. The bond paths (BP), shown with solid green lines, are the trajectories along which the electron density is at the maximum between two nuclei and passes through the bond critical point. These graphs show several interactions between hydrogens and electronegative atoms through the formation of hydrogen bonds. This kind of interaction appears within all the structures analyzed in this work. Besides, interactions between H_3AsO_4 molecules are presented in the one-side interaction mode. This set of interactions can lead to a stabilization of the system, as seen in Table 1.

Table 1 presents Free Energy values for the Chi-[As] adsorption process, considering the global and successive adsorption routes described in Eqs. (1) and (2). The global adsorption process represents the adsorption of a total number of arsenic molecules originating from the isolated chitosan moiety. In contrast, the successive adsorption process denotes the addition of one H_3AsO_4 initiating from a chitosan molecule already containing an absorbed arsenic molecule. The most stable process is, in fact, the successive adsorption of two acid molecules by one side of the polymer, which could be attributed to the larger number of interactions presented in the one-side interaction complex.

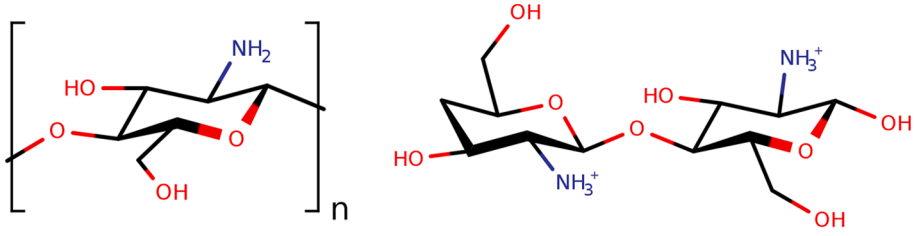

Fig. 1. A) on the left is the chemical structure of chitosan. b) at the right, the model is employed in dft calculations. amine groups were protonated to simulate ph = 1.

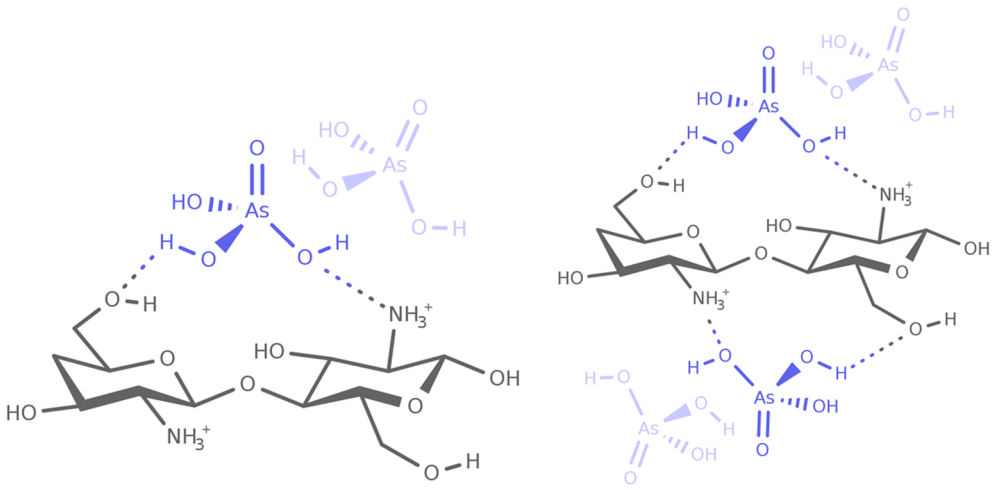

Fig. 2. Chi-As interaction modes observed in QM calculations. On the left, one-side interaction: arsenic molecules interact only on one side of the chitosan rings. On the right, both-side interactions: arsenic molecules approximate on both sides of the rings, producing a "sandwich" configuration. Light purple molecules indicate that more H_3AsO_4 can approach the chitosan substructure. Dotted lines represent schematic interaction.

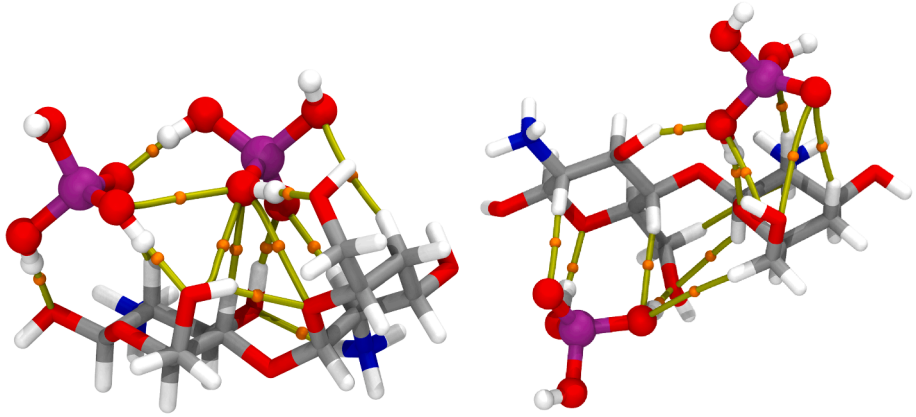

Fig. 3. Molecular graphs for a) One-side and b) Both-side interaction in the $Chi(H_3AsO_4)_2$ system. Orange dots depict the bond critical points. Ring a cage critical points are hidden.

Table 1
Global and successive ΔG (in kcal/mol) for systems with different accommodation patterns of the arsenic acid on chitosan.

H_3AsO_4 molecules	One-side interaction		Both-side interaction	
	Global ΔG	Successive ΔG	Global ΔG	Successive ΔG
1	6.1	6.1	6.1	6.1
2	−0.9	−7.1	12.2	6.1
3	5.8	6.7	8.2	9.1
4	16.3	10.5	9.7	4.0

The system reaches greater stabilization when it already has some arsenic molecules attached. Nevertheless, these interactions show small free energy values, which indicate the weak nature of the interactions.

(1) The global process where $n >= 1$

$$Chi + nH_3AsO_4 \rightarrow Chi(H_3AsO_4)_n \quad (1)$$

(2) And the successive adsorption process where $m >= 0$

$$Chi(H_3AsO_4)_m + H_3AsO_4 \rightarrow Chi(H_3AsO_4)_{m+1} \quad (2)$$

3.2. Evolution of Chi-As interactions

We simulated the polypropylene-chitosan + arsenic model described in Section 2 to study the dynamic evolution of the Chi-As interactions. A visual image of the adsorption process is essential to understanding the whole dynamic of the system. With this in mind, the propagated trajectory containing 181 K frames was analyzed through a DBScan clustering algorithm to obtain the representative conformations of the complete process. Six representative structures are shown in Fig. 4.

As discussed in section 3.1, the most stable process corresponds to $Chi(H_3AsO_4)_2$ formation in a one-side interaction. For this reason, at the beginning of the MD simulation, 12 H_3AsO_4 molecules were placed around 3 Å of the chitosan chain. Thus, 3 chitosan dimmers interact with 12 arsenic molecules, forming the complex PP-$Chi_3(H_3AsO_4)_{12}$. This structural arrangement is supported by experimental evidence concerning the predominant interaction between As and Chi in complex matrices. [12,56,57] At the beginning of the simulation, all arsenic molecules are found close to the chitosan chain. Across the trajectory, the molecules redistribute on top of the model, steadily forming a first interaction sphere between arsenic and chitosan, followed by a second sphere where H_3AsO_4 molecules interact directly with the first sphere, a similar array found by El Kaim Billah and coworkers [21]. This configuration closely resembles the structures presented in the DFT modeling section.

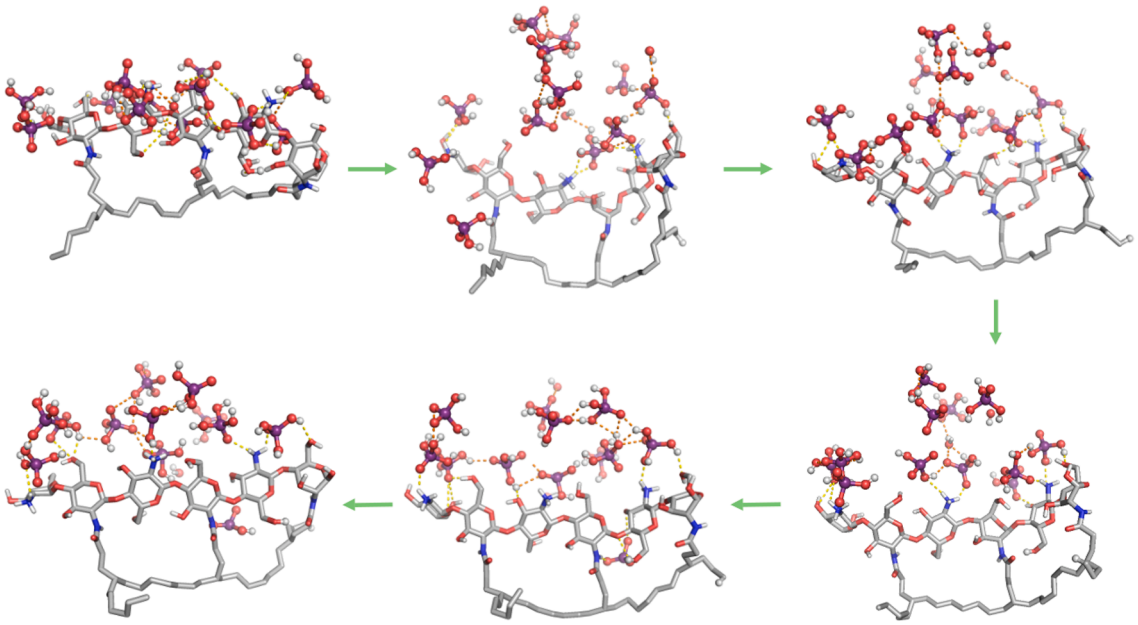

Fig. 4. Representative structures for the structural change during the MD trajectory. Dotted orange lines illustrate the [As]–[As] interaction; dotted yellow lines illustrate the Chi-[As] interaction.

In contrast with the static QM calculations, several proton exchanges are visualized during the propagation of molecular dynamics. Acid protons are interchanges between H_3AsO_4 and water molecules of the solvent. However, protons attached to $-NH_3^+$ groups do not interchange, as they are involved in the Chi-As interactions. Applying the same clustering method, the most representative structure of the whole trajectory was obtained. This configuration is shown in Fig. 5. The molecular graph of that conformation was calculated employing a wave function, which was calculated at the same level of theory (wB97X-D3/Def2-TZVP).

The molecular graph in Fig. 5b reveals the intricate structure formed atop the membrane. It can be seen that several bond paths are evident between arsenic and chitosan molecules. Here, diverse kinds of intermolecular interactions are exhibited, such as hydrogen bonds between arsenic and amino or hydroxyl groups, as reported experimentally [20], but also O—O interactions, and even H—H interactions. [56].

Considering the dynamic nature of the simulation, a structural analysis was performed for the whole propagated trajectory. The system was divided into i) an aliphatic carbon chain, ii) a chitosan chain, and iii) H_3AsO_4 molecules. Fig. 6 presents the calculated RMSD of the three different sections of the system. After 40 ps, the aliphatic chain is partially stabilized, and only a brief change is observed around 110 ps, corresponding to a conformational change of a brief chain folding. However, because of the conformation restriction of the chitosan polymer, the aliphatic chain returns to a linear conformation. This confirms

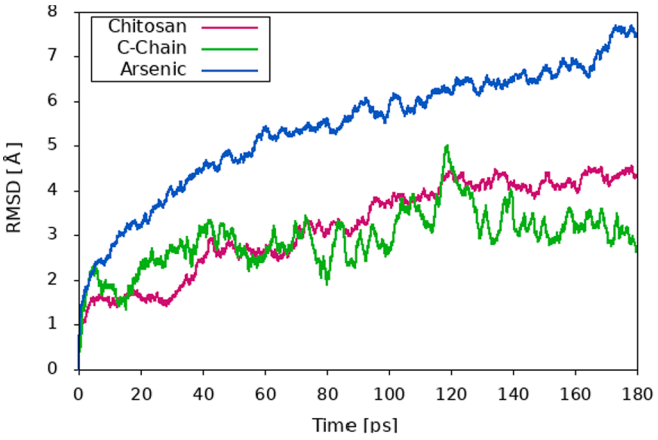

Fig. 6. Calculated RMSD for different sections within the model.

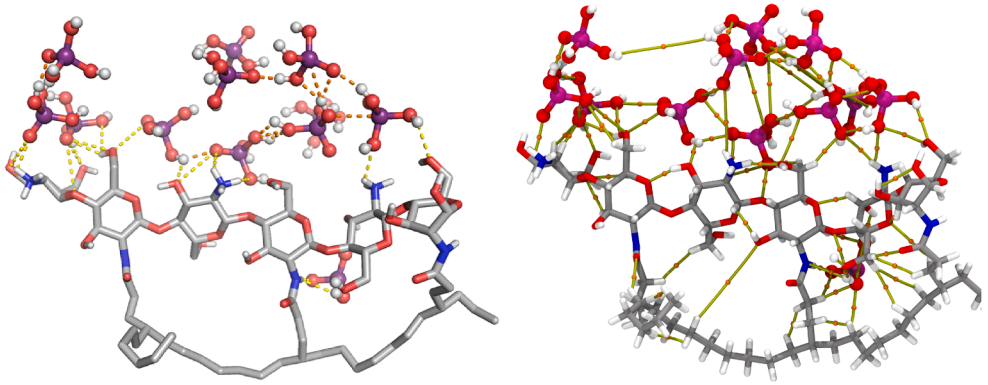

Fig. 5. a) A representative membrane structure was derived from the entire md trajectory using a clustering method. only some bonded interactions are depicted. b) molecular graph of the same system, depicting the whole set of as-as and chi-[as] interactions.

that significant chemical interactions with the arsenic molecule do not occur in this membrane area. The aliphatic chain only serves as a scaffold that provides structure to the membrane.

In contrast, RMSD for the chitosan chain slowly increases. It presents an abrupt change after 40 ps and a steady increment through the simulation. In the same way, the arsenic molecules diffuse through the polymer as expressed by the quasi-lineal change in the RMSD.

The molecular graph shows that the interactions between arsenic molecules and chitosan structures are primarily hydrogen bonds, as theoretical [10,21,45] and experimental data suggested [20,56]. For this reason, the number of hydrogen bonds between the chitosan chain and acid molecules was calculated and depicted in Fig. 7. In the first 20 ps, numerous interactions were observed, attributed to the initial placement of the H_3AsO_4 molecules. However, as the simulation propagates, the count of hydrogen bonds between chitosan and arsenic molecules decreases, stabilizing at around three bonds, neglecting the interactions among arsenic molecules. Once the system is relaxed, the number of hydrogen bonds fluctuates. It can be seen that around 110 ps, the number of hydrogen bonds between chitosan and arsenic diminishes, which can be related to the temporary change of the aliphatic chain structure. Considering the interaction between arsenic molecules, including the [As]-[As] contacts, the overall number of bonds is bigger, fluctuating around 6. This indicates that the system presents interactions between the biopolymer and the chitosan, but also interactions between arsenic molecules are essential to understanding the entire adsorption process.

To better understand the structural arrangement governing the intermolecular interactions in the adsorption process, the radial distribution functions (RDF) were calculated and shown in Fig. 8. Interactions between electronegative and hydrogen atoms were considered for both chitosan and arsenic molecules: 1) hydrogens from chitosan with oxygens from arsenic, Chi(H)–As(O) and 2) electronegative chitosan atoms with hydrogen atoms from H_3AsO_4, Chi(N,O)–As(H). In both distributions, a prominent peak occurs at approximately 1 Å, suggesting the presence of a well-defined first interaction shell. However, two additional peaks become clear in the Chi(H)–As(O) distribution. This suggests the formation of a second arsenic sphere over the chitosan. Therefore, the adsorption process of the arsenic over the chitosan occurs through a first interaction sphere formation, forming hydrogen bond interactions between chitosan and arsenic. After that, another

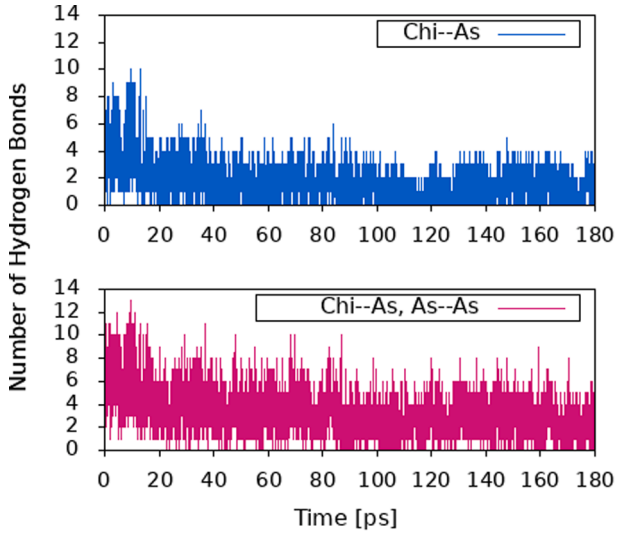

Fig. 7. Number of bonds calculated between the arsenic molecules and the chitosan moiety. The distance for donor–acceptor interactions was established at 3.5 Å, with an angle cutoff of 20°. Top: Hydrogen bonds between chitosan and arsenic moieties. Bottom: Hydrogen bonds between chitosan–arsenic and arsenic–arsenic molecules.

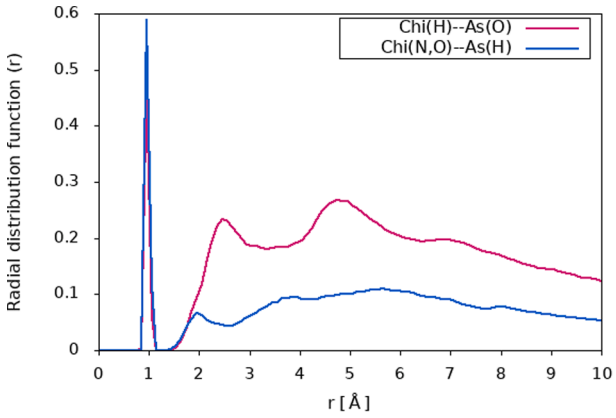

Fig. 8. The radial distribution function for the arsenic-membrane interactions.

interaction shell is formed between arsenic molecules through hydrogen bonds, as discussed above.

Díaz-Gómez et al. [58] have shown that the magnitude of the potential energy density at a BCP, $V(\mathbf{r}_{BCP})$, is directly linked to the interatomic interaction energy. The total interaction energy results from the summation of $V(\mathbf{r}_{BCP})$ at each Bond Critical Point, weighted by a constant that depends on the interaction as expressed in Eq. (1). The constant is 0.5 for hydrogen bonds determined empirically [52] and 0.433 for other weak interactions [58]. Table 2 depicts key properties of the interactions presented in representative systems. The complex Chi $(H_3AsO_4)_2$ was selected for the static DFT model due to its stabilization in the one-side configuration. Analysis of Chi$(H_3AsO_4)_2$ in both-side configuration was also conducted for comparison.

$$\Delta E_{int} \sum_{HB} 0.5V(rBCP) + \sum_{A\ldots B} 0.433V(rBCP) \quad (1)$$

Considering the molecular dynamic simulation, a representative structure for the PP-Chi$_3$$(H_3AsO_4)_{12}$ system was chosen. The count of interactions was done using the number of bond critical points along bond paths between the membrane and substrate atoms. The two Chi $(H_3AsO_4)_2$ models observe equal interactions. However, the both-side configuration lacks interaction between arsenic molecules, as shown in Fig. 3b. In both arrangements, the hydrogen bond interactions are predominant. Although the number of interactions is the same, the sum of the electronic density in the BCPs differs, being larger in the one-sided structure. For both $\sum\rho(\boldsymbol{r}BCP)$ and ΔE_{int} quantities, the [As]-[As] interactions provoke important changes in the total values.

The proportion of interaction types significantly influences ΔE_{int} values. The larger value for the one-side structure nearly doubles that presented in the both-side configuration. This is attributed to the stabilizing effect of [As]-[As] interaction. The same behavior was observed in the adsorption energy presented in Table 1. There is a relationship between the count of interactions within arsenic moieties and the decrease in the interaction energy. In turn, the PP-Chi$_3$$(H_3AsO_4)_{12}$ system presents a significant increase in the count of interactions in both Chi-[As] and [As]-[As] parts. The molecular dynamics simulation explores multiple conformations where arsenic molecules interact with the chitosan moiety and other H_3AsO_4 molecules. This way, the total number of interactions is five times larger than that in the isolated Chi $(H_3AsO_4)_2$ structure. It also can be seen that the larger contributions in the analyzed properties appear due to the interaction between arsenic molecules.

Therefore, it is proposed that the most crucial phenomena during the arsenic adsorption on top of the modified membrane are the [As]-[As] interactions. As the adsorption progresses, some arsenic molecules interact directly with the membrane, inducing system stabilization. Nevertheless, the process follows the energy stabilization gained through interactions of other arsenic molecules with those already

Table 2
Interaction energy and total electron density at BCP for the interaction between chitosan and arsenic molecules.

Model	Number of interactions			$\sum\rho(\mathbf{r}BCP)$ [a.u.]			ΔE_{int} [kcal/mol]		
	Chi-[As] (Hbond/Other)	[As]-[As](Hbond/Other)	Total(Hbond/Other)	Chi-[As]	[As]-[As]	Total	Chi-[As]	[As]-[As]	Total
$Chi(H_3AsO_4)_2$ *One-Side*	8/2	1/1	9/3 = 12	0.219	0.063	0.282	−61.6	−20.7	−82.2
$Chi(H_3AsO_4)_2$ *Both-Side*	10/2	0/0	10/2 = 12	0.181	0.000	0.181	−45.7	0.0	−45.7
PP-$Chi_3(H_3AsO_4)_{12}$	18/13	10/18	28/31 = 59	0.315	0.553	0.868	−63.9	−243.0	−307.9

absorbed. In this manner, the membrane can achieve a stable structure formed by at least two H_3AsO_4 shells atop the chitosan moiety.

4. Conclusions

The adsorption of arsenic onto a chitosan modified membrane is a complex process. Computational modeling provides valuable information about the intricate interaction at a molecular level. The study presented here reveals some insight into the adsorption reaction. The initial step involves interactions between arsenic molecules and electronegative atoms by forming hydrogen bonds. The DFT static calculations show that the adsorption energy is only an exergonic process when two H_3AsO_4 molecules are involved for each chitosan dimmer. The magnitude of the free adsorption energy denotes that weak interactions are involved during the process. Using this model, the most stable structure was observed for $Chi(H_3AsO_4)_2$ in a one-side conformation. In this configuration, the arsenic molecules interact only on the side of the chitosan rings. In contrast, both-side conformation presents a chitosan moiety in between arsenic molecules. On the other hand, molecular dynamics simulations were useful for studying the dynamics during arsenic adsorption. The process involves the formation of two layers. The primary layer features direct interactions between the chitosan moiety and H_3AsO_4 molecules, whereas the secondary layer presents arsenic interactions with each other and the initial layer. Interestingly, the arsenic-arsenic interactions within the secondary layer are crucial in structure stabilization. At the same time, the overall membrane structure remains almost unadulterated during the process. Analysis of specific molecular interactions through computational chemistry can provide valuable insights into the membrane–substrate. The results of this study support the activity of new material developed in our group that demonstrated the ability to remove arsenic (V) in 75 % removal.

CRediT authorship contribution statement

Brandon Meza-González: Writing – review & editing, Writing – original draft, Visualization, Validation, Methodology, Investigation, Formal analysis. **Mariela Molina Jacinto:** Writing – review & editing, Conceptualization. **Leonardo Brito-Flores:** Visualization, Validation, Software, Investigation. **Fernando Cortes-Guzman:** Writing – review & editing, Writing – original draft, Project administration, Methodology, Funding acquisition, Formal analysis, Conceptualization. **Rosa María Gómez-Espinosa:** Methodology, Conceptualization.

Declaration of competing interest

The authors declare that they have no known competing financial interests or personal relationships that could have appeared to influence the work reported in this paper.

Data availability

Data will be made available on request.

Acknowledgments

The authors thank DGTIC-UNAM (LANCAD-UNAM-DGTIC-194) for the computer time and CONAHCyT (CF2019-1561802/2020), DGAPA-UNAM (IN207822) and UAEM (6983/2024CIB) for financial support. BMG, MMJ, and LBF also thank CONAHCyT for the financial support (Grant 660455, 758332, and 1187346).

Appendix A. Supplementary data

Supplementary data to this article can be found online at https://doi.org/10.1016/j.chemphys.2024.112276.

References

[1] P.K. Jha, P. Tripathi, Groundw. Sustain. Dev. 13 (2021) 100576.
[2] J.O. Fatoki, J.A. Badmus, J. Hazard. Mater. Adv. 5 (2022) 100052.
[3] J. Mahlknecht, I. Aguilar-Barajas, P. Farias, P.S.K. Knappett, J.A. Torres-Martínez, J. Hoogesteger, R.H. Lara, R.A. Ramírez-Mendoza, A. Mora, Sci. Total Environ. 857 (2023) 159347.
[4] M.T. Alarcón-Herrera, D.A. Martin-Alarcon, M. Gutiérrez, L. Reynoso-Cuevas, A. Martín-Domínguez, M.A. Olmos-Márquez, J. Bundschuh, Sci. Total Environ. 698 (2020) 134168.
[5] C.C. Osuna-Martínez, M.A. Armienta, M.E. Bergés-Tiznado, F. Páez-Osuna, Sci. Total Environ. 752 (2021) 142062.
[6] N.R. Nicomel, K. Leus, K. Folens, P. Van Der Voort, G. Du Laing, Int. J. Environ. Res. Public Health 13 (2015) ijerph13010062.
[7] M.B. Shakoor, N.K. Niazi, I. Bibi, M. Shahid, Z.A. Saqib, M.F. Nawaz, S.M. Shaheen, H. Wang, D.C.W. Tsang, J. Bundschuh, Y.S. Ok, J. Rinklebe, Environ. Int. 123 (2019) 567.
[8] P. Lu, C. Zhu, Environ. Earth Sci. 62 (2011) 1673.
[9] L.N. Pincus, A.W. Lounsbury, J.B. Zimmerman, Acc. Chem. Res. 52 (2019) 1206.
[10] L.N. Pincus, P.V. Petrović, I.S. Gonzalez, E. Stavitski, Z.S. Fishman, H.E. Rudel, P. T. Anastas, J.B. Zimmerman, Chem. Eng. J. 412 (2021) 128582.
[11] L. Hao, M. Liu, N. Wang, G. Li, RSC Adv. 8 (2018) 39545.
[12] H. Zeng, Y. Yu, F. Wang, J. Zhang, D. Li, Colloids Surf. A Physicochem. Eng. Asp. 585 (2020) 124036.
[13] A. Ayub, Z.A. Raza, Int. J. Biol. Macromol. 192 (2021) 1196.
[14] J.J. García-García, R.M. Gómez-Espinosa, R.N. Rangel, R.R. Romero, G.R. Morales, Environ. Sci. Pollut. Res. Int. 29 (2022) 1909.
[15] K.C.M. Kwok, L.F. Koong, G. Chen, G. McKay, J. Colloid Interface Sci. 416 (2014) 1.
[16] D. Cortés-Arriagada, A. Toro-Labbé, RSC Adv. 6 (2016) 28500.
[17] R. Srivastava, A. Kommu, N. Sinha, J.K. Singh, Mol. Simul. 43 (2017) 985.
[18] S. Borah, P.P. Kumar, J. Phys. Chem. B 122 (2018) 3153.
[19] M. Yahyaei, F. Mehrnejad, H. Naderi-Manesh, A.H. Rezayan, Eur. J. Pharm. Sci. 107 (2017) 126.
[20] G. Cabrera-Barjas, F. Gallardo, A. Nesic, E. Taboada, A. Marican, Y. Mirabal-Gallardo, F. Avila-Salas, N. Delgado, M. de Armas-Ricard, O. Valdes, J. Environ. Chem. Eng. 8 (2020) 104355.
[21] R. El Kaim Billah, Md. Aminul Islam, H. Lgaz, E.C. Lima, Y. Abdellaoui, Y. Rakhila, O. Goudali, H. Majdoubi, A.A. Alrashdi, M. Agunaou, A. Soufiane, Arab. J. Chem. 15 (2022) 104123.
[22] A. Yadav, S.S. Dindorkar, S.B. Ramisetti, N. Sinha, J. Water Process Eng. 46 (2022) 102653.
[23] M. Rinaudo, Prog. Polym. Sci. 31 (2006) 603.
[24] P. Pracht, F. Bohle, S. Grimme, Phys. Chem. Chem. Phys. 22 (2020) 7169.
[25] J.-D. Chai, M. Head-Gordon, Phys. Chem. Chem. Phys. 10 (2008) 6615.
[26] V. Barone, M. Cossi, J. Phys. Chem. A 102 (1998) 1995.
[27] F. Neese, F. Wennmohs, U. Becker, C. Riplinger, J. Chem. Phys. 152 (2020) 224108.
[28] R.M. Kumar, J.V. Sundar, V. Subramanian, Int. J. Hydrogen Energy 37 (2012) 16070.
[29] Y. Wang, J. Liu, S. Tang, Z. Dai, R. Jin, Struct. Chem. 27 (2016) 897.
[30] C. Halsey-Moore, P. Jena, J.T. McLeskey, Comput. Theor. Chem. 1162 (2019) 112506.
[31] U. Salzner, A. Aydin, J. Chem. Theory Comput. 7 (2011) 2568.
[32] M. Wierzbicka, I. Bylińska, C. Czaplewski, W. Wiczk, RSC Adv. 5 (2015) 29294.
[33] J. Frau, D. Glossman-Mitnik, Molecules 23 (2018).
[34] T.A. Keith, AIMAll, TK Gristmill Software, Overland Park KS, USA, 2016.
[35] R.F.W. Bader, Atoms in molecules: a quantum theory, Oxford University Press, Oxford UK, 1990.
[36] S. Grimme, C. Bannwarth, P. Shushkov, J. Chem. Theory Comput. 13 (2017) 1989.

[37] T.D. Kühne, M. Iannuzzi, M. Del Ben, V.V. Rybkin, P. Seewald, F. Stein, T. Laino, R. Z. Khaliullin, O. Schütt, F. Schiffmann, D. Golze, J. Wilhelm, S. Chulkov, M. H. Bani-Hashemian, V. Weber, U. Borštnik, M. Taillefumier, A.S. Jakobovits, A. Lazzaro, H. Pabst, J. Hutter, J. Chem. Phys. 152 (2020) 194103.
[38] J. Kohn, S. Spicher, M. Bursch, S. Grimme, Chem. Commun. 58 (2021) 258.
[39] J. Řezáč, J.J.P. Stewart, J. Chem. Phys. 158 (2023) 044118.
[40] C. Plett, S. Grimme, Angew. Chem. Int. Ed 62 (2023) e202214477.
[41] L. Wilbraham, E. Berardo, L. Turcani, K.E. Jelfs, M.A. Zwijnenburg, J. Chem. Inf. Model. 58 (2018) 2450.
[42] M.A. Kelland, J. Pomicpic, R. Ghosh, S. Abdel-Azeim, Energy Fuels 36 (2022) 3088.
[43] Q.H. Zhang, N. Xu, Z.N. Jiang, H.F. Liu, G.A. Zhang, J. Colloid Interface Sci. 640 (2023) 1052.
[44] N.T.T. Ha, N.T.K. Giang, N.N. Ha, P.T. Lan, Mol. Simul. 49 (2023) 1303.
[45] L.A. Zemskova, D.K. Shlyk, A.V. Voit, N.N. Barinov, Russ. Chem. Bull. 68 (2019) 9.
[46] A.A. Menazea, H.A. Ezzat, W. Omara, O.H. Basyouni, S.A. Ibrahim, A.A. Mohamed, W. Tawfik, M.A. Ibrahim, Comput. Theor. Chem. 1189 (2020) 112980.
[47] H.S. Adhikari, A. Garai, P.N. Yadav, Carbohydr. Res. 526 (2023) 108796.
[48] D.R. Roe, T.E. Cheatham, J. Chem. Theory Comput. 9 (2013) 3084.
[49] W. Humphrey, A. Dalke, K. Schulten, J. Mol. Graph. 14 (1996) 33.
[50] T.P.M.G.S. Schrödinger, LLC, Pymol, n.d.
[51] R.F.W. Bader, H. Essén, J. Chem. Phys. 80 (1984) 1943.
[52] E. Espinosa, E. Molins, C. Lecomte, Chem. Phys. Lett. 285 (1998) 170.
[53] O.A. Zhikol, O.V. Shishkin, K.A. Lyssenko, J. Leszczynski, J. Chem. Phys. 122 (2005) 144104.
[54] R. Parthasarathi, V. Subramanian, Struct. Chem. 16 (2005) 243.
[55] C.F. Matta, J. Comput. Chem. 35 (2014) 1165.
[56] T.G. Asere, S. Mincke, J. De Clercq, K. Verbeken, D.A. Tessema, F. Fufa, C. V. Stevens, G. Du Laing, Int. J. Environ. Res. Public Health 14 (2017).
[57] A.I.A. Sherlala, A.A.A. Raman, M.M. Bello, A. Buthiyappan, J. Environ. Manage. 246 (2019) 547.
[58] D.G. Díaz-Gómez, R. Galindo-Murillo, F. Cortés-Guzmán, ChemPhysChem 18 (2017) 1909.